



High-resolution NMR of anisotropic samples with spinning away from the magic angle

Dimitris Sakellariou, Carlos A. Meriles, Rachel W. Martin, Alexander Pines *

*Materials Science Division, Lawrence Berkeley National Laboratory, and Department of Chemistry,
University of California, Berkeley, CA 94720, USA*

Received 15 April 2003; in final form 27 June 2003

Published online: 25 July 2003

Abstract

High-resolution NMR of anisotropic samples is typically performed by spinning the sample around an axis at the ‘magic’ angle of 54.7° with the static magnetic field. Geometric and engineering constraints often prevent spinning at this specific angle. Implementations of magic angle field rotation are extremely demanding due to power requirements or an inaccessible geometry. We present a methodology for taking the magic out of MAS while still obtaining both isotropic and anisotropic spectral information during sample spinning or field rotation at arbitrary angles. Using projected-MAS, we obtained resolved scaled isotropic chemical shifts in inhomogeneously broadened spinning samples. Published by Elsevier B.V.

1. Introduction

The introduction of magic angle spinning (MAS) in NMR [1,2], allowed high-resolution spectra of samples subject to anisotropic line broadening. Under fast spinning of the sample around an axis that makes a specific angle of $\theta_m = \arctan \sqrt{2} \approx 54.7^\circ$ with the static magnetic field B_0 , called the magic angle, a significant line narrowing occurs. The time dependent spatial part of the anisotropic interactions averages over a rotor period and the time independent component

is canceled by the choice of the angle. Currently, MAS is applied routinely in most high-resolution solid-state NMR experiments, and spinning frequencies continue to increase dramatically with increasing B_0 [3].

The idea, first proposed by Andrew and Eades [4], of spinning the field at the magic angle represents an alternative for static samples located inside (in situ) or outside (ex situ) of the magnet and has recently been the focus of considerable attention [5,6]. Here the constraint of reaching the magic angle represents serious engineering problems, since in the case of spinning the field electromagnetically or rotating a permanent magnet, the required power increases substantially with the angle [7]. In addition, there are cases where even mechanically spinning the sample exactly at the

* Corresponding author. Fax: +1-510-486-5744.
E-mail address: pines@cchem.berkeley.edu (A. Pines).

magic angle represents a problem due to possible geometrical constraints (e.g., elongated samples that cannot be spun inside the bore of a superconducting magnet), or even induced disorder (e.g., liquid crystals [8]).

Here we present a method named projected-MAS which is based on switched angle spinning (SAS) in order to obtain high-resolution two-dimensional spectra containing isotropic–anisotropic correlations. Correlations between isotropic and anisotropic information have been previously obtained using a variety of related methods, including switched angle spinning (SAS) [9–12], dynamic angle spinning (DAS) [13,14], and variable angle correlation spectroscopy (VACSYS) [15]. In the SAS experiment, an evolution period and/or chemical shift refocusing at angle θ_1 (which is often 0 or 90°) is followed by detection at the magic angle. This results in the isotropic spectrum along the F_2 dimension being correlated to anisotropic chemical shift or dipolar lineshapes obtained along F_1 , providing valuable information that would be lost in a simple isotropic MAS experiment. This method has been used to measure chemical shift anisotropies, dipolar couplings and hence internuclear distances in solids and in liquid crystals. Magic angle hopping [16] or magic angle turning (MAT) [17] experiments use rotor synchronized pulses to produce an isotropic spectrum in one dimension and a manifold of sidebands resembling the full powder pattern in the other. MAT experiments can be used to obtain isotropic information in situations where fast MAS is not practical or desirable. DAS was developed in order to obtain high-resolution NMR of quadrupolar nuclei. In this method, the first- and second-order quadrupolar broadening are removed by spinning sequentially at two complementary angles such that the terms of rank two and four in the Hamiltonian are both removed. The spins evolve at an angle θ_1 for time t_1 , and then at θ_2 for time t_2 . If the spinning angles and the evolution times are chosen correctly, evolution under the rank two and rank four terms during the second evolution period will cancel that from the first, giving an isotropic spectrum in the indirect dimension, correlated with the anisotropic lineshape obtained at θ_2 in the direct dimension. Although this technique does not

specifically involve the use of the magic angle, it still requires careful choice of complementary angles in order to obtain the full isotropic–anisotropic correlation. In contrast to the other correlation methods, which make use of specific spinning angles, if not the magic angle itself, VACSYS produces its isotropic–anisotropic correlations by sampling a wide range of angles in separate one-dimensional acquisitions. After data processing and reconstruction [18] two-dimensional spectra are obtained relating the isotropic chemical shifts to the chemical shift anisotropy.

In implementation, projected-MAS (p-MAS) is similar to previously developed methods for producing isotropic–anisotropic correlations; in fact it should be noted that all of the experiments discussed here can be performed with essentially the same instrumentation. However, our goals here are quite different; we are interested in recording the full isotropic and anisotropic spectral information by spinning the sample or the magnetic field around axes making angles with the static magnetic field away from the magic angle. The purpose of the p-MAS experiment is to remove the constraint of having to choose the spinning angle based on the spin mathematics: instead the angle can be chosen based on other factors, such as power requirements or sample geometry. Since the Larmor frequencies are much higher than the spinning frequencies, the adiabatic limit is satisfied and spinning the field is essentially equivalent to spinning the sample. The power requirements of spinning a field become less stringent when the angle of rotation is lower. From Fig. 1, one can estimate that stronger magnetic fields generated by electromagnets can be rotated faster at the expense of a smaller angle of rotation. Keeping in mind the existing techniques, our goal here is to develop the methodology for the equivalent off-magic angle field spinning experiments.

In this Letter, the first implementation of p-MAS is shown. Spectra of different samples subject to susceptibility broadening are recorded while spinning the sample away from the magic angle. The two-dimensional spectra provide correlations between the anisotropic and the scaled isotropic chemical shifts. Extensions of the method to one-dimensional p-MAS and projected-magic

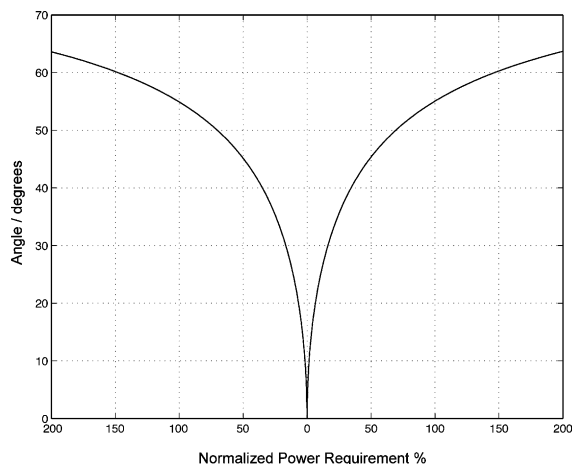


Fig. 1. Diagram representing the power requirements necessary to obtain an electromagnetically spinning magnetic field at a given angle. Three perpendicular pairs of coils are assumed, one of which is static and the other two drive oscillating currents. The normalization is made assuming that 100% is the power needed for the magic angle. From the diagram one can appreciate the dramatic drop in power requirements when the angle is close to zero.

angle turning versions are discussed together with the limitations of the approach.

2. Projected-magic angle spinning

In what follows we treat samples characterized by inhomogeneous [19] anisotropic broadening, including mechanisms such as magnetic susceptibility, heteronuclear dipolar coupling and chemical shift anisotropy. All of these interactions are assumed to transform like rank two spatial tensors upon sample rotation¹. The spin Hamiltonian for such spin systems can be written as

$$H(t; \theta) = \sum_{m=-2}^2 \exp(-im\omega_r t) H_m(\theta). \quad (1)$$

Making the assumption that the spinning frequency is much higher than the anisotropic

broadening, only the term that corresponds to $m = 0$ is relevant. This term is responsible for the width of the centerband and can be expressed as

$$H_0(\theta) = H_{\text{iso}} + \mathcal{P}_2(\cos \theta) H_{\text{aniso}}, \quad (2)$$

where $\mathcal{P}_2(\cos \theta)$ is the rank two Legendre polynomial. The two-dimensional p-MAS experiment consists of a free evolution period during time t_1 with the sample spinning at an angle θ_1 , followed by the acquisition during time t_2 at an angle θ_2 . The pulse sequence is depicted schematically in Fig. 2a. The hopping of the rotor from θ_1 to θ_2 and its stabilization takes some finite time of the order of several milliseconds. Thus, between the two evolution periods a storage period τ is inserted in order to preserve the transverse signal as longitudinal magnetization, which decays more slowly. Proper phase cycling [14] selects the coherence pathways shown in Fig. 2b allowing frequency sign discrimination in both dimensions. This pulse scheme leads to a two-dimensional spectrum of correlations between two anisotropic dimensions, with width determined by the values of the respective Legendre polynomials for θ_1 and θ_2 . Nevertheless, resolution is recovered with an appropriate projection or ‘shearing’ which produces isotropic chemical shifts scaled by a scaling factor λ . The slope of the projection depends on the ratio of the polynomials for the two angles. The narrow ridges in the two-dimensional frequency spectrum are equivalent to echoes of the anisotropic part of the Hamiltonian in the time domain. This can be easily seen from the one-dimensional equivalent of the sequence presented in Fig. 2c. There the π pulses refocus the evolution of the magnetization giving rise to echoes of the chemical shift anisotropy for the proper choice of τ_1 and τ_2 . In this pulse sequence the switching between the angles θ_1 and θ_2 is assumed to be infinitely rapid, a limit that might be easier to achieve for field spinning compared to sample spinning. The 2D data can also be sheared and represented in the form of ordinary isotropic–anisotropic correlations. In order to observe a refocusing of the anisotropy, the anisotropic evolution (dephasing) must be the same in both dimensions

$$\tau_1 \mathcal{P}_2(\cos \theta_1) = \tau_2 \mathcal{P}_2(\cos \theta_2). \quad (3)$$

¹ The line broadening coming from homogeneous or higher rank components in the Hamiltonian will be discussed later in this Letter.

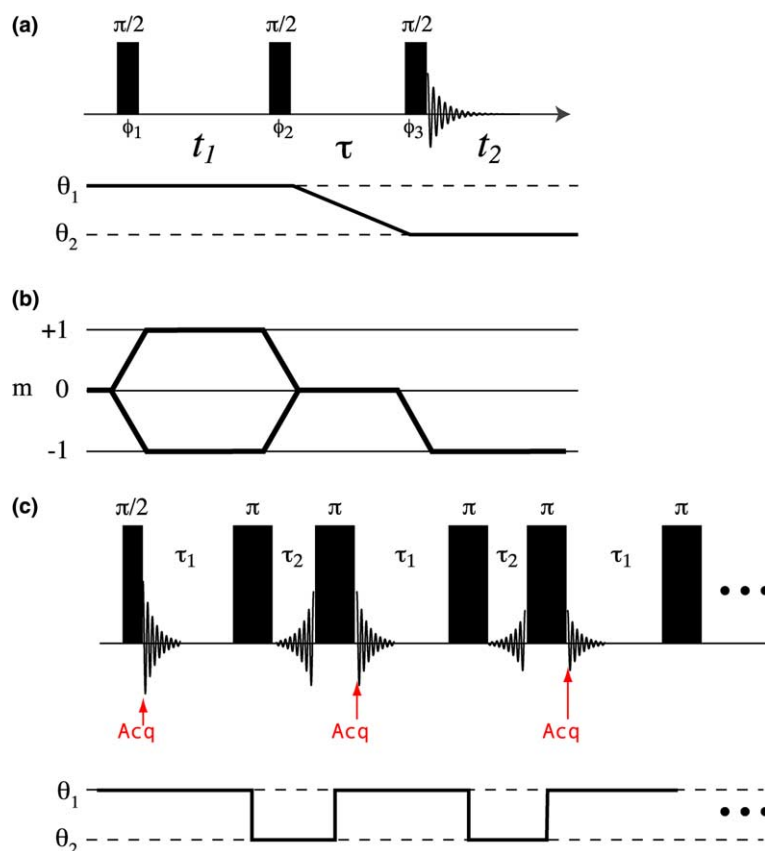


Fig. 2. (a) Pulse sequence for switched angle spinning experiments. The phase cycling [14] is such that only the coherence pathway diagram presented in (b) contributes to observable signal. (c) One-dimensional equivalent sequence. Switching of the spinning angles is assumed infinitely fast and stroboscopic point-by-point acquisition takes place at the echoes of the chemical shift anisotropy.

On the other hand, the net evolution after time $\tau_1 + \tau_2$ of the isotropic chemical shift is

$$\begin{aligned} \sigma_{\text{iso}}(\tau_1 - \tau_2) &= \sigma_{\text{iso}}(\tau_1 + \tau_2) \frac{\tau_1 - \tau_2}{\tau_1 + \tau_2} \\ &= \sigma_{\text{iso}}(\tau_1 + \tau_2) \frac{1 - \tau_1/\tau_2}{1 + \tau_1/\tau_2}, \end{aligned} \quad (4)$$

and using Eq. (3), one can calculate the scaling factor from the refocusing conditions to be

$$\lambda = \frac{\mathcal{P}_2(\cos \theta_1) - \mathcal{P}_2(\cos \theta_2)}{\mathcal{P}_2(\cos \theta_1) + \mathcal{P}_2(\cos \theta_2)}. \quad (5)$$

A representation of the scaling factor for different pairs of spinning angles is shown in Fig. 3. The resolution is dependent not only on the difference between the switching angles, but also on the absolute value of these angles, rendering the scaling

extremely small for angles close to zero degrees. Of course, to the extent that the residual linewidth also scales with the angle this is not a problem. We mention here that related two-dimensional correlations experiments of amorphous solids exhibiting inhomogeneous broadening, can yield highly resolved projections (see [20] and references therein).

3. Experiments

All data were acquired on a Chemagnetics Infinity Spectrometer operating at 500 MHz ^1H frequency, using an extensively modified Varian 4 mm SAS probe. The probe design is such that the solenoidal radio-frequency coil stays parallel to the

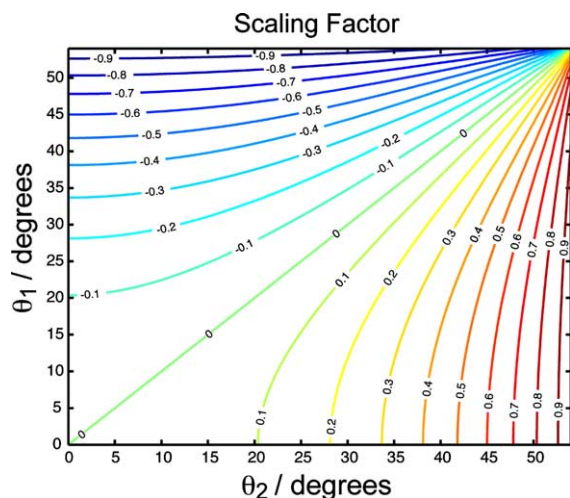


Fig. 3. Scaling factor for the isotropic chemical shift interaction as a function of the two switching angles. Notice how quickly the scaling factor drops in the region close to zero degrees, making p-MAS particularly challenging.

rotor at any angle, rendering the excitation and detection at an angle close to zero degrees not efficient. The filling factor and the rf homogeneity are comparable to any commercial MAS probe. The samples were spun at approximately 7 kHz and the pulse sequence of Fig. 2a was implemented using a τ period of 60–80 ms for the stator switching and stabilization depending on the difference of the switching angles [21]. The precision of the angle setting was estimated to be around 0.1° . The magic angle was calibrated by maximizing the number of spinning sidebands on the spectrum of polycrystalline KBr.

Two samples exhibiting proton anisotropic susceptibility broadening were analyzed. A sample, used in the literature [22] as a model for susceptibility broadening in living tissues was prepared by using glass beads with sizes between 210 and 250 μm . The beads were soaked with water and mineral oil and then packed inside the rotor. The spectrum of the static sample has a linewidth of 7 kHz, while the residual linewidth under MAS was 80 Hz. The second sample was a Berea sandstone rock sample also containing water and mineral oil. The residual linewidth of this sample under MAS was 500 Hz. The origin of this linewidth, though not fully understood, could be

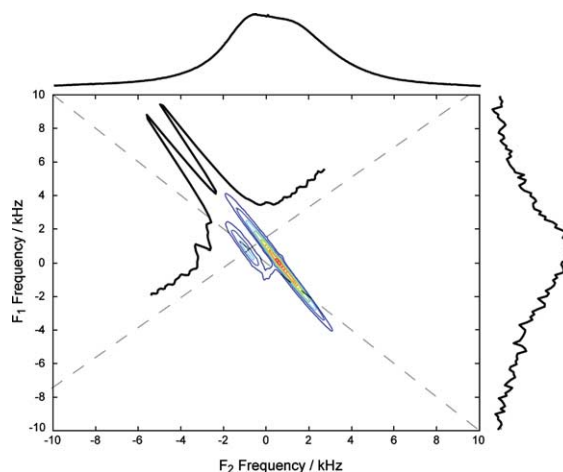


Fig. 4. Two-dimensional p-MAS spectrum of a sample containing glass beads saturated with water and mineral oil. The angles θ_1 and θ_2 were set to 4.5° and 25.0° , respectively. 128 t_1 increments with 32 averaged scans each were recorded. The switching delay τ was set to 50 ms. The experimental scaling factor was 0.15. The total experimental time was 18 min.

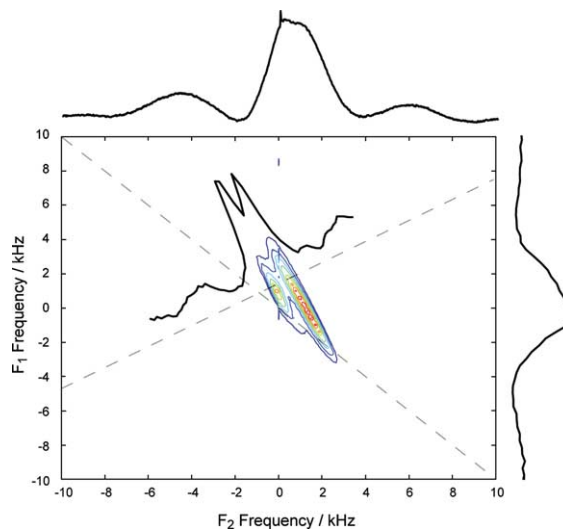


Fig. 5. Two-dimensional p-MAS spectrum of a Berea rock sample containing water and mineral oil. The angles θ_1 and θ_2 were set to 33.0° and 47.5° and the switching delay was equal to 70 ms. The two isotropic resonances can be easily identified. The experimental scaling factor was 0.4.

due to other broadening mechanisms such as T_2 relaxation and/or other higher rank components of the magnetic susceptibility. In particular, the

distribution of pore sizes could lead to a distribution of isotropic susceptibility that cannot be averaged away [23]. The contribution of the rank four component of the susceptibility is averaged out by MAS as shown in [3], but other sample shape dependent terms could, in principle, be present [23]. In our experiments such terms proved to be rather small.

In Fig. 4, we present an experimental 2D p-MAS spectrum of the beads sample, together with the projections along the two anisotropic dimensions. The angles were set to $\theta_1 = 4.5^\circ$ and $\theta_2 = 26^\circ$, providing a theoretical scaling factor of 0.16 for the isotropic chemical shift. After a shearing transformation one can obtain a trace displaying the isotropic spectrum as shown. The two resonances from water (left) and mineral oil (right) can be clearly distinguished.

The experimental data after 2D Fourier transform are presented in Fig. 5 for the sample of Berea sandstone rock saturated with water and mineral oil. MAS spectra have been recorded in the literature and show a dramatic increase in resolution over those of the static sample [24]. In Fig. 5 the angle θ_1 was set to 33.0° and θ_2 to 47.5° . We also recovered the isotropic information while using $\theta_1 = 4.5^\circ$ and $\theta_2 = 47.5^\circ$ (data not shown). These experimentally observed scaling values compare well with the ones obtained from Eq. (5) of 0.67 and 0.47, respectively. The residual linewidth of this sample is much greater than that of the beads sample, making the experiment more sensitive to the scaling of the isotropic chemical shift.

4. Discussion

One condition of the previous treatment is that the spinning frequency was considered greater than the magnitude of the anisotropic interaction. As a result the time dependent parts of the Hamiltonian were not included and spinning sidebands are absent. In the case of field spinning, estimates of the achievable spinning frequencies depend on the size of the rotating components and thus on the angle of the conical trajectory of the total field. However, we do not expect frequencies much

higher than several kilohertz to be easily achievable, rendering the problem of spectral resolution non-trivial because of the presence of spinning sidebands. Rotor synchronized techniques, such as magic angle hopping [16] or turning [17,25,26], have been developed in the past and could be easily combined into the framework of experiments away from the magic angle. This type of techniques eliminate the presence of sidebands even in the case of very slow spinning [27]. This does not represent a serious problem for the technique and we plan to show that with the appropriate hardware such combined techniques can recover the isotropic information even in the presence of the very slow spinning. Work in building a synchronized switched angle turning probe is in progress.

Another experimental issue we encountered involved the design of the probe. The use of a solenoidal coil which is coaxial with the rotor excludes efficient excitation and detection at angles close to zero. Other designs that allow excitation and detection of a spinning sample at zero degrees have been developed in the past e.g., [21], and we are currently working on improving our apparatus to include such designs. For the future application of spinning the magnetic field off the magic angle and close to zero however, this does not present a problem. In this case one would expect an increase in signal to noise since rotating close to zero would allow us to use higher total magnetic fields. On the other hand, the magnitude of the scaling factor compared to the residual homogeneous linewidth is expected to be the limiting factor of this approach. A future extension of this technique to one-dimensional schemes, as shown in Fig. 2c, is envisaged in our laboratory. Since it would require stroboscopic acquisition during fast reorientation of the spinning axis, such 1D versions would be particularly well adapted for field spinning experiments. Along the same ideas, VACSYS [15] could also offer an interesting alternative. Its limited angle version is currently under development.

We have presented a proof of principle that spinning away from the magic angle, and even close to zero degrees with respect to B_0 , can in some cases dramatically improve the resolution and produce isotropic–anisotropic correlation

spectra. Projected magic angle spinning can be applied in cases where spinning the sample or the field at the magic angle is inaccessible. Further developments along the previously mentioned lines are in progress and will be described in future work.

Acknowledgements

This work was supported by the Director, Office of Science, Office of Basic Energy Sciences, Materials Sciences Division, of the US Department of Energy under Contract No. DE-AC03-76SF00098.

References

- [1] E.R. Andrew, A. Bradbury, R.G. Eades, *Nature* 182 (1958) 1659.
- [2] I.J. Lowe, *Phys. Rev. Lett.* 2 (1959) 285.
- [3] A. Samoson, T. Tuhem, Z. Gan, *Solid State Nucl. Magn. Reson.* 20 (2001) 130.
- [4] E.R. Andrew, R.G. Eades, *Discuss. Faraday Soc.* 34 (1962) 38.
- [5] C.A. Meriles, D. Sakellariou, H. Heise, A.J. Moulé, A. Pines, *Science* 293 (2001) 82.
- [6] C.A. Meriles, D. Sakellariou, A. Pines, *Chem. Phys. Lett.* 358 (2002) 391.
- [7] R.C. Gupta, *Indian J. Pure Appl. Phys.* 13 (1975) 39.
- [8] J. Courtieu, D.W. Alderman, D.M. Grant, J.P. Bayles, *J. Chem. Phys.* 77 (1982) 723.
- [9] A. Bax, N.M. Szeverenyi, G.E. Maciel, *J. Magn. Reson.* 55 (1983) 494.
- [10] T. Terao, T. Fujii, T. Onodera, A. Saika, *Chem. Phys. Lett.* 107 (1984) 145.
- [11] T. Terao, H. Miura, A. Saika, *J. Chem. Phys.* 85 (1986) 3816.
- [12] A.C. Kolbert, P.J. Grandinetti, M. Baldwin, S.B. Prusiner, A. Pines, *J. Phys. Chem.* 98 (1994) 7936.
- [13] A. Llor, J. Virlet, *Chem. Phys. Lett.* 152 (1988) 248.
- [14] K.T. Mueller, B.Q. Sun, G.C. Chingas, J.W. Zwanziger, T. Terao, A. Pines, *J. Magn. Reson.* 86 (1990) 470.
- [15] L. Frydman, G.C. Chingas, Y.K. Lee, P.J. Grandinetti, M.A. Eastman, G.A. Barrall, A. Pines, *J. Chem. Phys.* 97 (1992) 4800.
- [16] A. Bax, N.M. Szeverenyi, G.E. Maciel, *J. Magn. Reson.* 52 (1983) 147.
- [17] J.Z. Hu, D.W. Alderman, C. Ye, R.J. Pugmire, D.M. Grant, *J. Magn. Reson. A* 105 (1993) 82.
- [18] Y.K. Lee, R.L. Vold, G.L. Hoatson, Y.Y. Lin, A. Pines, *J. Magn. Reson. A* 112 (1995) 112.
- [19] M.M. Maricq, J.S. Waugh, *J. Chem. Phys.* 70 (1979) 3300.
- [20] D. Sakellariou, S.P. Brown, A. Lesage, S. Hediger, M. Bardet, A. Meriles, A. Pines, L. Emsley, *J. Am. Chem. Soc.* 125 (2003) 4376.
- [21] K.T. Mueller, G.C. Chingas, A. Pines, *Rev. Sci. Instrum.* 62 (1991) 1445.
- [22] J.Z. Hu, R.A. Wind, *J. Magn. Reson.* 159 (2002) 92.
- [23] M. Alla, E. Lippmaa, *Chem. Phys. Lett.* 87 (1982) 30.
- [24] T.M. de Swiet, M. Tomaselli, M.D. Hürlimann, A. Pines, *J. Magn. Reson.* 133 (1998) 385.
- [25] J.Z. Hu, W. Wang, F. Liu, M.S. Solum, D.W. Alderman, R.J. Pugmire, D.M. Grant, *J. Magn. Reson. A* 113 (1995) 210.
- [26] E.A. Hill, J.P. Yesinowski, *J. Chem. Phys.* 106 (1997) 8650.
- [27] J.Z. Hu, D.N. Rommereim, R.A. Wind, *Magn. Reson. Med.* 47 (2002) 829.